Advanced methods based on active thermography for fast inspection of cast iron components used in the automotive industry

Fabrizio Freni[1], Roberto Marsili[2], Roberto Montanini[1], Antonino Quattrocchi[1], Annamaria Di Giacomo[1] and Gianluca Rossi[2]
1 University of Messina, Italy, {ffreni, rmontanini, aquattrocchi, adigiacomo}@unime.it
2 University of Perugia, Italy, {roberto.marsili, gianluca.rossi}@unipg.it

Abstract

This paper explores the application of vibrothermography with ultrasonic excitation for the detection and quantification of flaws in industrial cast iron components. The use of amplitude modulated ultrasonic heat generation allowed selective response of defected area, since the defect itself is turned into a local thermal wave emitter. Due to the very fast cycle time (< 30 s/part), the method could potentially be applied for 100% quality control of cast parts. After a brief description of the measurement technique and experimental setup used to carry out the tests, main results and discussion are reported. Most emphasis has been addressed to assess the influence of different operative parameters on defect's detection capability as well as accurate sizing of the discontinuity.

1. Introduction

In the last decades, the industrial interest on the development of advanced non-destructive techniques for the qualification of materials and products has been increased noticeably. As example, the investigation of internal discontinuities such as voids, porosity, shrinkage, slag and inclusions in cast iron turbo parts is today carried out routinely using x-ray and γ-ray radiography (1). In parallel, ultrasounds represent another characterization technique that has been extensively studied for application as quality control tool in casting production (2).

The above mentioned techniques can be considered as well-known methods, and devices based on such a technologies are today widely available in commerce. In recent years, researchers are pointing their efforts towards the development of new non-destructive testing (NDT) methods which allow for fast, no contact and reliable manufacturing quality control. Among these, active infrared thermography (AIT) is one of the most promising one. In AIT, thermal waves are used to excite the specimen in order to induce significant temperature differences witnessing the presence of subsurface anomalies (3). A large variety of sources, which include either optical, electromagnetic or acoustic excitation, have been successfully experimented to generate a thermal path into the part to be inspected. Meanwhile, signal to noise ratio and detection capability have been drastically improved using lock-in thermography (4-5), where the process of bandwidth reduction makes use of the complete coded information contained in the sequence of thermograms recorded at one single modulation frequency.

Among the different excitation sources that can be used to deposit heat on the target surface, vibrothermography (VT) uses ultrasound-generated heat as defect detection mechanism. The basic principle is based on theory that as defects may be areas where mechanical damping and friction losses primarily take place, the vibro-acoustic energy is converted into heat mainly in defects than in sound areas, resulting in a defect selective dark field method (6-7).
This paper explores the use of ultrasound excited lock-in thermography (ULT) (8) as an effective method for the inspection of cast iron turbocharger components. Due to its exceptionally fast response, the proposed method could potentially be applied for 100% inspection of complex castings parts, with notably time and economic saving when compared to well established NDT techniques. The attention is first focused on evaluating the influence of different working parameters (carrier frequency, modulation frequency, ultrasound excitation power, number of heating cycles) on defect's detection capability and on the optimization of the experimental setup (choice of the "best parameters set") for the specific application. Finally, phase thermal images obtained on both defected and sound parts are reported and a fast algorithm for defect's sizing is presented.

2. Experimental set-up

A batch of several defected and sound cast iron turbo housing samples (figure 1a), with two different geometries (namely type 1 and type 2), were provided by a leading Italian foundry, holding 30% of the world-wide market in castings for turbochargers. Each sample was first examined by x-ray radiography and 3D computed tomography and then subjected to thermographic NDE.
The experimental setup used in our study basically consists of a high resolution infrared camera, a ultrasound generation unit, a pneumatically-driven coupling system and a control unit for software lock-in. The infrared camera (FLIR Titanium 560 M) has a 640 x 512 pixels InSb FPA detector working in the MWIR (3.6 – 5.1 μm) spectral band and was equipped with a 50 mm F2 focal length lens. The NETD was stated by the manufacturer to be better than 20 mK at ambient temperature. A 2.2 kW digital ultrasound generator coupled to a pneumatically controlled resonance unit including a damped piezo-ceramic converter, a booster and a sonotrode were used to optimize ultrasound injection into the sample (figure 1 b).

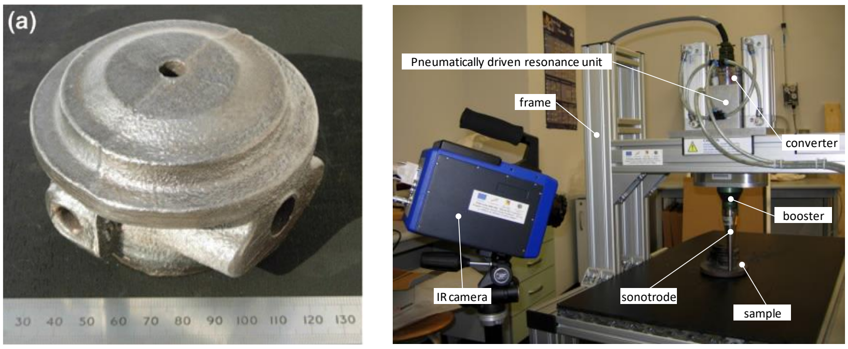

a) b)

Figure 1. a) cast iron turbo housing sample (type 1) and b) experimental set-up for ultrasound excited thermography

The allowable range for the excitation frequency generated by the ultrasonic converter was approximately 15 kHz – 25 kHz with adjustable amplitude from 0% to 100%. The carrier frequency was modulated using low-frequency sinusoidal signals (lock-in mode) set between 0.01 Hz and 1 Hz. The temperature modulation at the surface was analysed by tuning the IR camera acquisition to the frequency of amplitude modulation. The DisplayIMG ver.2.6 software (Edevis GmbH, Germany) was used to control the acquisition and record thermal images. Special care was reserved to ensure efficient acoustic coupling and impedance matching between the sonotrode tip and cast sample surface, which is not planar: best results were obtained by interposing a 3 mm thick Teflon strip between the two coupling surfaces.

3. Experimental results

3.1. Definition of the working parameters: sensitivity analysis

Preliminary tests were carried out in order to investigate the influence of different working parameters on the normalized phase contrast, which has been defined as follows:

$$C^n(t_f) = \frac{\Delta\varphi(t_f)}{\varphi_s(t_f)} = \frac{\varphi_{def}(t_f) - \varphi_s(t_f)}{\varphi_s(t_f)} \tag{1}$$

where $\varphi_{def}(t_f)$ and $\varphi_s(t_f)$ are the average phase values of defected and sound regions, measured at the end time tf of the thermal process over a small circular area (4 mm diameter) of the thermogram.
The following parameters were considered:
1. excitation frequency f_c (15 kHz ... 25 kHz, with 0.5 kHz step increment)
2. number of heating periods N (1 ... 20)
3. nominal amplitude of ultrasound power P% (1 ... 30%)
4. frequency of amplitude modulation fm (0.01 Hz ... 1 Hz)

Sensitivity analyses were then carried out by varying each single parameter keeping the other ones constant.
Figure 2a shows the thermo-acoustic spectrum computed over the defected area by wobbling the excitation frequency from 15 kHz to 25 kHz. The thermo-acoustic spectrum can guide the selection of optimal excitation frequency for lock-in measurements.

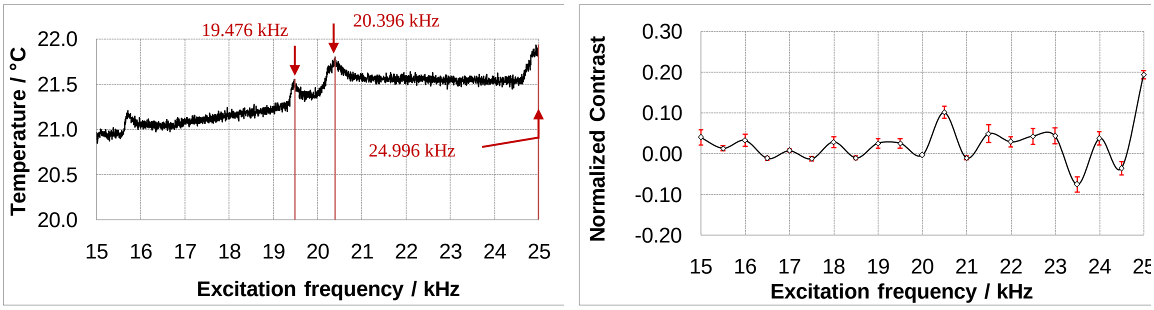

Figure 2. a) thermo-acoustic spectrum after frequency wobbling and b) normalized contrast (± standard deviation) as a function of the excitation frequency measured in lock-in mode with 0.05 Hz amplitude modulation (N=1, $P_{\%}$=12)

By observing the graph, three resonance frequencies causing significant temperature increments are observed at 19476 Hz, 20396 Hz and 24996 Hz, respectively. Figure 2b shows the effect of the excitation frequency on the normalized contrast in lock-in mode. These tests were done by fixing all the parameters (f_m=0.05 Hz, N=1, P%=12) while rising the excitation frequency step by step up to 25 kHz. For each frequency, tests were repeated three times. By comparing the two plots of figures 2a and 2b, a good correlation can be highlighted, although not all the resonance peaks observed in the thermo-acoustic spectrum actually lead to an appreciable phase contrast in amplitude modulated measurements. One reason of this behaviour might be attributed to the different duration of the excitation between the two experimental tests: the multy-frequency test, in fact, takes 100 s to sweep the whole frequency range, while lock-in measurements were modulated at 0.05 Hz (test duration 20 s). Hence, the overall heating of the sample was actually higher in the second case, leading to a considerable reduction of either amplitude or phase contrast. In addition, monofrequent excitation can produce superimposed temperature patterns caused by standing elastic waves due to vibrational resonance matching (e.g., 23.5 kHz point data in figure 2b). Both results indicate 25 kHz as the optimal excitation frequency (maximum temperature rise, maximum normalized contrast), hence this value was used to carried out all the following tests.
The effect of the number of heating periods on defect detection is reported in figure 3a. These tests were performed with fm=0.05 Hz, fc=25 kHz and P%=12. As practical NDT routines based on ULT have to be implemented along a production line, this parameter is important, since it is directly related to the total cycle time of the conformity verification test. By increasing the number of cycles from 1 to 15, the normalized contrast computed over the defect area rises twofold. At the same time, the obtained results provide evidence that the discontinuity can be reliably detected even if a single modulation period is used (cycle time 20 s).

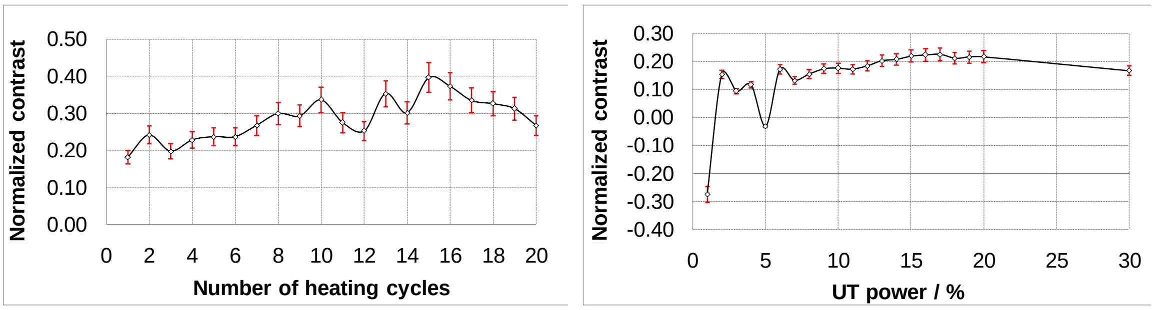

Figure 3. a) effect of the number of heating cycles on defect detection (f_m=0.05 Hz, f_c=25 kHz, $P_{\%}$=12) and b) normalized contrast as a function of percentage ultrasound power (errors bars showing ± standard deviation on three repeated measurements) (f_m=0.05 Hz, f_c=25 kHz, N=1)

The effect of nominal amplitude of ultrasound power is illustrated in figure 3b. These tests were performed with fm=0.05 Hz, fc=25 kHz and N=1.This parameter has little influence on the normalized phase contrast, providing an adequate (> 6%) amplitude intensity is transferred to the part. Hence, as far as applications on casting are concerned, our results suggest that high power excitation is not necessary to identify the discontinuity, thus reducing the risk of local damage due to a significant thermal load during the ultrasonic excitation.

The correlation between the lock-in frequency and the normalized contrast is investigated in figure 4. These tests were performed with f_c=25 kHz, P%=12 and N=1. As it can be observed, the phase angle difference reaches a maximum for modulation frequencies between 0.04 Hz and 0.1 Hz. By assuming a one-dimensional model for the thermal wave field (7), the depth range of the defect may be estimated as (being α = 0.15 cm^2/s the material thermal diffusivity, $\omega = 2\pi f$ the angular frequency, μ the thermal diffusion length)

$$z \cong 1.8\mu = 1.8\sqrt{\frac{2\alpha}{\omega}} \tag{2}$$

which yields a defect depth extension between 12.4 mm and 19.7 mm. These values are roughly 2.5 times larger than the actual ones, leading to the conclusion that the use of a simplified model for thermal wave field prediction is not adequate in this case and more complex numerical models have to be implemented in order to estimate defect depth.

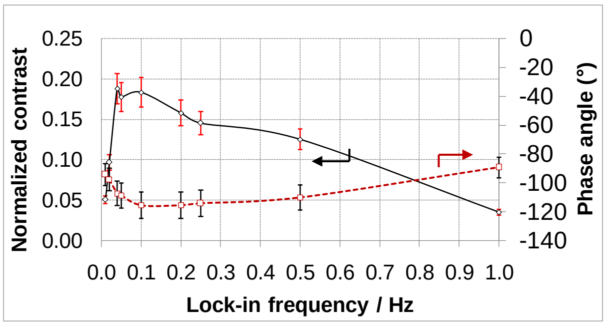

Figure 4. Effect of the modulation frequency on normalized contrast computed over the defected area and phase angle plot (errors bars showing ± standard deviation on three repeated measurements) (f_c=25 kHz, $P_{\%}$=12, N=1)

3.2. Defects detection

On the ground of preliminary sensitivity tests reported in the previous section, the following set of optimal parameters was selected: f_c=25 kHz, f_m=0.05 Hz, P%=12 and N=1.

The following figures highlight the main results obtained by examining several defected and sound samples of two distinct types of cast iron turbocharger housings, having a slightly different geometry and identified as type 1 and type 2, respectively. The samples were furnished as cast and were not subjected to neither further processing nor surface finishing, so that the applicability of the proposed ULT technique along the production line could be assessed.

Figure 5 refers to the type 1 housing geometry. The overall cycle time of a typical test was about 30 s, including positioning of the sample on the test bench. The sample 1a presents a solidification shrinkage void (lack of fusion) subsurface discontinuity in the front view that was easily detected by ultrasound excited lock-in thermography. The unfilled region, located along the circumferential transition between the two cylindrical volumes that form the upper part of the turbo housing, is about 5 mm wide and extends to a depth of 7.8 mm, as empathized by CT slices computed by means of an x-ray tomographic scan (further details are given in the figure's caption). The minimum distance to the measured surface is roughly 2 mm. For comparison purpose, phase thermograms obtained on a sound sample (1b) belonging to the same production batch are also reported in the figure.

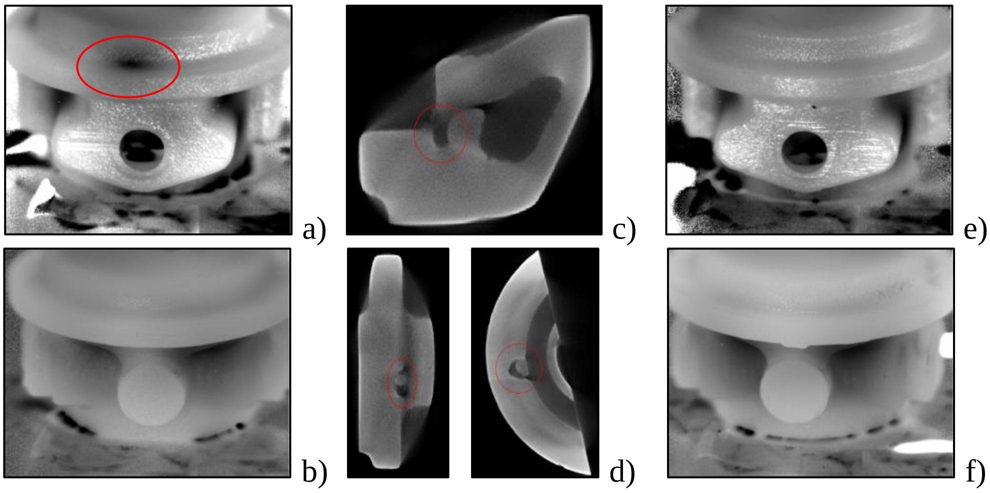

Figure 5. ULT nondestructive testing results on type 1 cast iron turbo components (coupling: PTFE, modulation frequency: 0.05 Hz, UT excitation frequency: 25 kHz, UT amplitude: 12%, number of preheating/heating cycles:0/1): a) gray level phase image of sample 1a (defected, front view); b) gray level phase image of sample 1a (sound, back view); c-d) CT slices of sample 1a computed by means of variable focus 225 kV x-ray tomography (Vacc = 160 kV; Aacc = 1.50 mA; focus spot = 800 mm): radial section (top), vertical section (bottom left) and horizontal section (bottom right); e) gray level phase image of sample 1b (sound, front view); f) gray level phase image of sample 1b (sound, back view)

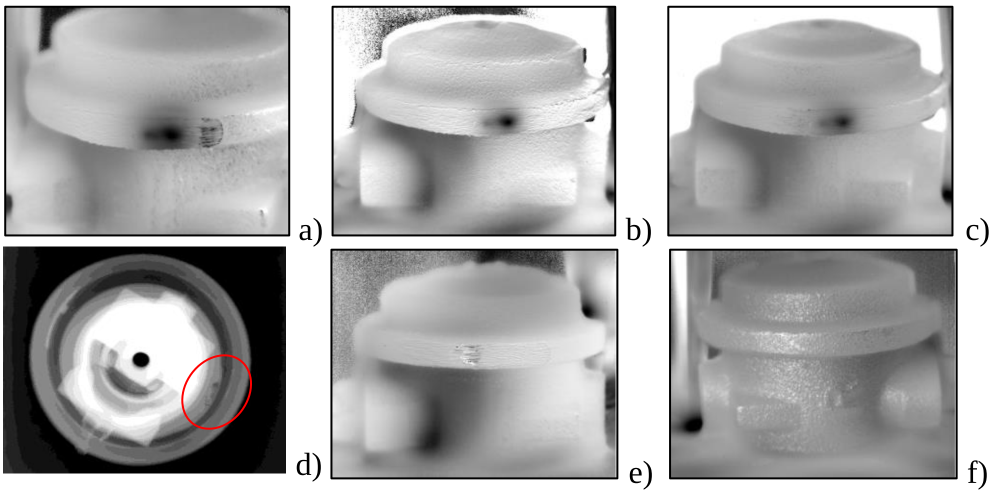

Figure 6. ULT nondestructive testing results on type 2 cast iron turbo components (coupling: PTFE, UT excitation frequency: 22 kHz, UT amplitude: 12%, number of preheating/heating cycles:0/1): a) gray level phase image of sample 2a obtained with 0.2 Hz modulation (defected, front view); b) gray level phase image of sample 2a obtained with 0.1 Hz modulation (defected, front view); c) gray level phase image of sample 2a obtained with 0.05 Hz modulation (defected, front view); d) γ-ray radiography of sample 1a showing the subsurface multi-segmented macro porosity; e) gray level phase image of sample 2b obtained with 0.05 Hz modulation (sound, front view); f) gray level phase image of sample 2a obtained with 0.05 Hz modulation (sound, back view)

Figure 6 refers to the type 2 housing geometry. Similar sensitivity tests as those reported in the section 4.1 for the type 1 geometry were performed in order to find an optimal set of working parameters (fc=22 kHz, fm=0.05-0.2 Hz, P%=12 and N=1). The overall cycle time was typically around 20 s, including positioning of the sample on the test bench. The sample 2a presents a porosity discontinuity located on the larger diameter region of the turbo housing. The flaw, as confirmed by the □-ray radiography shown in the same figure, has multi-segmented spots that covers an area of about 11 mm width, at about 3.5 mm from the measured surface. Results are presented for slightly different values of the lock-in frequency to show how this parameter influences defect's detectability. In the same figure, phase thermograms of a sound sample (2b) belonging to the same production batch are shown for comparison.
It has to be noted that, although the results presented in this study clearly proved that ULT was able to identify the presence of defects in a reliable and repeatable way, it does not provide information about the nature of the discontinuity: defects of different origin in cast iron components, such as slag inclusions, cracking, porosity and solidification shrinkage voids, are likely to produce similar thermal signature.

3.3. Defects sizing

A simple yet effective semi-automatic method has been developed to process phase images for defect size assessment (figure 7). The algorithm, built up in the Matlab□ environment, works according to a histogram-based image segmentation based on iterative thresholding. Starting from the measured phase image, a region of interest (ROI) is first defined by the user. Then, the gray-level histogram of the windowed image is analysed and the image segmented using a "first tentative" threshold value. Hence the threshold TH is varied recursively to some extent and the results weighted using a knowledge matrix to search for an optimal TH value. The histogram-based algorithm can also be quickly adapted to process multiple frames. Hence, it can be used to compare several parametrized phase images to find out optimal working parameters for the specific application.

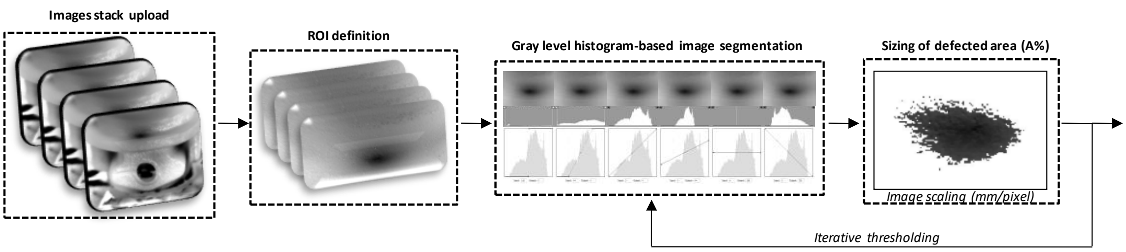

Fig. 7. Flow chart of the algorithm used for defect size assessment

5. Conclusions

This paper explored the use of ultrasound activated infrared thermography for quality control assessment in castings. The experimental approach is based on selective heating of inner flaws in cast iron turbo housings by means of high frequency ultrasonic waves modulated in amplitude by a lock-in sinusoidal signal. The effectiveness of the proposed measurement technique has been demonstrated throughout several examples showing reliable defect's detection of subsurface discontinuities located up to 3.5 mm depth. The overall cycle time was typically around 30 s, including positioning of the sample on the test bench. A simple and fast algorithm for defect's sizing based on automatic recognition of the gray levels distribution within the phase thermal image was also implemented for automatic defect sizing. The algorithm can process several images in few seconds, allowing the percentage defected area within the ROI to be estimated almost in real-time and user-defined acceptance/rejection criteria to be easily established. This is an important requisite for the practical implementation of this nondestructive testing technique in 100% quality control industrial protocols. Nevertheless, also drawbacks exist: the proposed technique failed in discriminating between discontinuities of different origin. In addition, more complex models for thermal wave field prediction than the simple one-dimensional one are compulsory for accurate defect's depth estimation.

References

1. RH Bossi, FA Iddings, GC Wheeler, "Nondestructive Testing Handbook", Third Edition: Volume 4, Radiographic Testing, The American Society for Nondestructive Testing, USA, 700 p., 2002.
2. F Lofaj, T Seldis, KF Nilsson, A Eriksson, "Ultrasonic Study of Defects in Ductile Cast Iron Inserts For Spent Nuclear Fuel Disposal", 9th European NDT Conference, September, 25-29, Berlin, 2006.
3. X Maldague, "Theory and practice of infrared technology for nondestructive testing", J. Wiley & Sons ed., New York, 684 pp, 2001.
4. GM Carlomagno, PG Berardi, "Unsteady Thermography in Non-Destructive Testing," in Proceedings of the 3rd Biannual Information Exchange, St. Louis/USA, pp 33–40, 1976.
5. G Busse, "Optoacoustic phase angle measurement for probing a metal", Appl. Phys. Lett. 35, pp 759–760, 1979.
6. R Montanini, F Freni, "Correlation between vibrational mode shapes and viscoelastic heat generation in vibrothermography", NDT&E International 58, pp 43-48, 2013.
7. R Montanini, F Freni, GL Rossi, "Quantitative evaluation of hidden defects in cast iron components using ultrasound activated lock-in vibrothermography", Review of Scientific Instruments 83(9), pp 094902-1/8, 2012.
8. Th Zweschper, A Dillenz, G Busse, "Ultrasound lockin thermography – a defect-selective NDT method for the inspection of aerospace structures", Insight 43(3), pp 173-9, 2001.